

**BRITISH GEOLOGICAL SURVEY  
TECHNICAL REPORT  
Mineralogy & Petrology Series**

**REPORT NO. WG/90/36**

**MINERALOGY AND PETROGRAPHY OF  
BOREHOLE SAMPLES TAKEN FROM  
LANDSLIPPED GAULT CLAY,  
SHAFTSBURY, DORSET**

**A J Bloodworth**

27 November 1990

*Geographical index*

Church Farm, Shaftsbury, Dorset ST 855 223

*Subject index*

Mudrock, smectite, geotechnical properties, shear plane, fabric analysis.

*Bibliographic reference*

**Bloodworth, A J.** 1990. Mineralogy and petrography of borehole samples taken from landslipped Gault Clay, Shaftsbury, Dorset.

*British Geological Survey  
Technical Report WG/90/36*

This report has been generated from a scanned image of the document with any blank pages removed at the scanning stage.  
Please be aware that the pagination and scales of diagrams or maps in the resulting report may not appear as in the original

**British Geological Survey**

**Mineral Sciences Group**

**Mineralogy and Petrology Report WG/90/36**

**MINERALOGY AND PETROGRAPHY OF BOREHOLE SAMPLES  
TAKEN FROM LANDSLIPPED GAULT CLAY, SHAFTSBURY,  
DORSET**

**A J Bloodworth**

**1. INTRODUCTION**

This report describes the mineralogy of shallow borehole material taken from the Gault Clay and part of the overlying Upper Greensand at Church Farm, west of Shaftsbury, Dorset. The investigation forms part of the Engineering Geology Group project 'Engineering properties of the Gault Clay'. This site was selected for detailed study because of the presence of low-angle landslips affecting both the Gault Clay and the overlying Cann Sand (Upper Greensand). The primary aim of the study was to assess the influence of mineralogy on the position of the slip plane. Whole-rock and clay mineralogy were determined in a total of 28 samples taken from two boreholes (Church Farm 1 and 2). Particularly detailed (cm-scale) sampling was carried out across the slip plane, which had been identified previously during logging of the core. Petrographic examination of a thin section cut across the slip plane was carried out in order to identify any sedimentological features which might have influenced the position of the slip plane, as well as to assess the effect of the slip on the mudrock fabric.

Hand-specimen descriptions of the samples are given in Table 1, together with depths and Mineral Sciences sample codes.

**2. LABORATORY METHODS**

Samples GC01-GC04 and GC10-GC18 were provided in bulk form by the Engineering Geology Group. Samples GC05-GC09 and samples GC18-GC28 were taken directly from undisturbed core. A further sample was cut across the estimated position of the shear plane in undisturbed core from borehole 2. This was used for preparation of a polished thin section.

Representative sub-samples were taken from the core material. These were dried at 55°C prior to hand-crushing by pestle and mortar. Approximately one-third of this material was then hammer-milled to pass a 125 µm screen and a portion micronized for

five minutes to provide a uniform particle size for whole-rock X-ray diffraction analysis.

The remaining two-thirds of the material was placed in a beaker and covered with distilled water, stirred and allowed to slough overnight. After further stirring the sample was then dispersed using an ultrasonic probe. Some samples showed a tendency to flocculate despite these treatments. Where this occurred, the supernatant was removed every few hours and replaced with distilled water until the suspension stabilized. A nominal  $<2\ \mu\text{m}$  fraction was then removed from the clay suspensions after a sedimentation time calculated according to Stokes' Law.

X-ray diffraction analysis was carried out using a Philips 1700 series automatic diffractometer. Co-K $\alpha$  radiation was used at 45 kV and 40 mA. Whole-rock (random powder) samples were examined over the angular scanning range  $3\text{-}50^\circ 2\theta$  at a speed of  $1.2^\circ 2\theta/\text{minute}$ , whilst  $<2\ \mu\text{m}$  (oriented clay) samples were scanned at a similar speed over the range  $1.5\text{-}32^\circ 2\theta$ .

Because of the likely influence of smectite on the geotechnical properties of the rock, this mineral was determined separately from surface area measurements using a procedure based on the monolayer adsorption of the polar organic reagent 2-ethoxyethanol. Smectite-group minerals have a much higher surface area than most other clay minerals and measurement of this property affords a means of determining the amount of smectite in mixed-mineral assemblages.

The polished thin section prepared from material taken from borehole 2 was examined by scanning electron microscope (SEM) using backscattered electron imaging (BSEM). Prior to examination by SEM, the polished sections were made electrically conductive by coating with a thin layer of carbon. BSEM analyses were undertaken using a Cambridge Instruments Stereoscan S250 Mark 1 scanning electron microscope fitted with a KE Developments 4-element solid-state backscatter electron detector. Mineral identification was aided by qualitative observation of energy-dispersive X-ray spectra facilitated by a Link Systems 860 series A energy-dispersive X-ray microanalysis system.

### **3. RESULTS AND DISCUSSION**

#### **3.1. Mineralogy**

Whole-rock and  $<2\ \mu\text{m}$  fraction mineralogy for each sample taken from boreholes 1 and 2 are given in Tables 2 and 3. Quartz is present throughout and small amounts of feldspar were detected in almost all samples. Non-silicates such as pyrite, calcite and gypsum are much more variable and these are absent entirely from the upper part of borehole 2. The clay mineral assemblage is similar throughout borehole 1 and the upper

part of borehole 2. The  $<2 \mu\text{m}$  fraction in these samples is dominated by smectite, with subordinate mica and minor kaolinite. The proportion of kaolinite relative to smectite and mica increases with depth in the lower part of borehole 2. Quartz and cristobalite were also detected in all  $<2 \mu\text{m}$  fractions examined. Typical diffraction traces illustrating these changes are shown in Figure 1.

Smectite values derived from surface area data are plotted against depth in Figures 2 and 3 (boreholes 1 and 2). Both boreholes show an increase in smectite content with depth toward the shear zone. Below the shear plane, smectite levels in borehole 2 abruptly decrease and stabilize. A repetition of this pattern is indicated in borehole 1, though there are insufficient samples from below the shear plane to confirm this. The similarity in smectite levels immediately above and below the shear plane in both boreholes is further illustrated by a plot of smectite concentration against distance from shear (Figure 4).

Vertical variations in mineralogy shown by the borehole material (particularly from borehole 2) are considered largely to be a reflection of the type and amount of sediment input. The effect of modern weathering processes also influences the mineral assemblage, though to a much lesser extent.

The quartz - feldspar - smectite - mica - kaolinite assemblage is typical of the Gault Clay and overlying Upper Greensand (Perrin, 1971). The decreasing levels of kaolinite and increasing levels of smectite in the clay mineral assemblage toward the top of the Gault has been noted elsewhere in Southern England and is considered to reflect a relative increase in the volcanogenic input to these sediments (Jeans *et al.*, 1982). Ash from contemporary acid or alkaline volcanism was introduced to the marine environment and became argillized to form smectite, giving rise to a distinctive smectite - mica assemblage which differs from the (detrital) kaolinite - mica assemblage which typifies the middle part of the Gault (Jeans *et al.*, 1982). Ash may have been introduced directly as air-fall material, or more likely, as accumulations transported into the sea by rivers draining ash-blanketed local land areas (so-called secondary bentonites). Increasing amounts of ash or argillized ash, mixed in with a continued input of 'normal' detrital material, would account for the gradational change in clay mineralogy seen in borehole 2. Localized 'highs' in smectite (10.58-10.70 m in borehole 1; 5.74-5.84 m in borehole 2) are likely to be the result of a temporary direct or indirect increase in input of volcanogenic material relative to 'normal' clastic sediment. The apparent decrease in smectite in samples taken from the top few metres of borehole 2 is a reflection of the overall increase in the proportion of coarse clastic material (principally quartz) in the sediment as the Upper Greensand facies became established.

In borehole 2, quartz appears to be related to levels of silt and sand-grade material and shows a clear increase across the Gault/Upper Greensand boundary at the top of the

sequence cored. The effect of modern weathering processes on the non-silicates present in these sediments is marked. The calcite / pyrite assemblage in samples from borehole 1 appears largely unaffected by oxidation. This contrasts strongly with material from the upper part of the Gault cut by borehole 2 at a much shallower depth. In these samples, pyrite and calcite are present in much lower concentrations or are absent entirely. The presence of gypsum in some of these samples suggests that oxidation of pyrite has taken place as a result of weathering, with subsequent reaction of acid groundwater with calcite to form secondary gypsum. These weathering processes do not appear to have any significant effect on the silicate component of these rocks.

### 3.2. Petrography

Petrographic analysis was carried out on a small sample (extending from 5.72 to 5.76 m) cut across the shear zone identified in during logging of borehole 2. The principal intention of the petrographic analysis of this material was to identify any primary (sedimentary) features which might influence the position of the shear plane, as well as to assess the effect of the shear on the fabric of the mudrock.

Petrographic analysis was undertaken principally using BSEM imaging. In this technique, image brightness is proportional to the average atomic number of the material, allowing the distribution of different minerals to be determined on the basis of chemical composition.

Plate 1 shows material typical of the upper portion of the section (approximately 8-10 mm above the estimated position of the shear plane). Angular and sub-angular sand-grade quartz grains are supported in a clay matrix, along with large mica flakes, sponge spicules and sand-grade glauconite grains. These observations confirm the results of X-ray diffraction analysis of samples taken from the upper part of borehole 2 and show similarity to Upper Greensand facies material elsewhere in Southern England (Jeans *et al.*, 1982). The fabric observed in this portion of the slide appears largely undisturbed by movement along the shear zone.

The increase in the proportion of clay minerals (particularly smectite) in the area immediately adjacent to the shear plane noted during X-ray diffraction analysis is also apparent from examination of the thin section. The strongly contrasting mineralogy and fabric in this area can be seen in Plate 2 which shows a 3 mm vertical section made up of a number of BSEM images taken at the same magnification. Figure 5 opposite summarizes important features shown by the composite photograph. The large number of shrinkage cracks in this portion of the slide is due to the relative decrease in the proportion of coarse clastic material such as quartz. Quartz grains are less abundant and are generally much smaller than those in Plate 1. Clay grade material is much more abundant. Several large glauconite are prominent and appear to be a feature of the clay-rich sediment below the sand, along with mica flakes and sponge spicules.

The textural differences between the sandy material and the more clay-rich sediment in the estimated position of the shear plane are very strong. Cracks in the section (which are black on the BSEM image) provide a useful indicator of particle orientation. The upper part of Plate 2 shows an extremely contorted clay matrix containing numerous clay pellets which vary considerably in size and shape. The internal structure of the pellets or clasts is sub-laminar and presumably represents the original fabric of the sediment prior to disturbance by the shear. The contrasting angles shown by this lamination between different clasts, along with the contorted matrix material, may reflect micro-scale rotational movements undergone during the slippage process. Clasts of undisturbed material ('ambient pellets'), persisting within random material formed by their degradation, are a relatively common feature of shear zones in clays (Morgenstern & Tchalenko, 1967).

The middle/lower portion of Plate 2 shows a zone of strongly oriented particles which is approximately 0.6 mm thick and probably corresponds with the position of the shear plane. The matrix in this zone is more uniform and particle orientation almost certainly reflects the direction of movement of the shear. The strong orientation of larger features such as glauconite pellets and mica flakes is particularly striking. Another area of contorted clay matrix containing undisturbed clay clasts can be seen immediately below this zone.

Narrow zones showing a strongly-oriented fabric bounding broader zones of random or contorted matrix material containing undisturbed clasts are commonly observed in sheared clays (Morgenstern & Tchalenko, 1967; Skempton & Petley, 1967). Clay showing strongly-oriented fabric is considered to mark the location of the principal displacement shear.

Because of the extreme disturbance of the fabric of the clay induced by the landslide movement, it was not possible to infer any primary sedimentary features which might have influenced the precise location of the shear.

#### **4. CONCLUSIONS**

Mineralogical analysis shows a clear relationship between the position of the shear plane and whole-rock smectite content, with the shear plane clearly following a zone of higher smectite values in both boreholes. These increase by some 10-15% in the immediate vicinity of the shear plane and both boreholes show a similar pattern in values up to a metre either side. Temporary increases in the proportion of acidic or alkaline volcanic ash, relative to 'normal' clastic material, were probably responsible for such small-scale vertical variations in smectite content. Detection of these variations requires relatively detailed (cm- scale) sampling of the borehole material.

Other than conspicuous variations in non-silicate mineralogy caused by the influence of surface weathering, the mineralogy of material taken from the two boreholes in the region of the shear is very similar. On this basis, it is possible to conclude that the horizons cut by the shear plane in both boreholes are very close (though not necessarily identical) stratigraphically.

The fabric of the clay in the section cut from borehole 2 has been very strongly influenced by movement(s) along the shear plane, with little or no trace of the original texture remaining. A narrow zone of strongly-oriented particles which may mark the precise position of the shear is surrounded by broader areas of contorted material within which fragments or clasts of undisturbed mudrock remain. These textures appear to be characteristic of sheared mudrocks which have been observed elsewhere.

*Acknowledgement:* Valuable advice on Gault Clay mineralogy and petrography from Mr R J Merriman is gratefully acknowledged.

#### REFERENCES

Jeans, C V, Merriman, R J, Mitchell, J G & Bland, D J (1982) Volcanic clays in the Cretaceous of Southern England and Northern Ireland. *Clay Minerals* **17**, 105-156.

Morgenstern, N R & Tchalenko, J S (1967) Microstructural observations on shear zones from slips in natural clays. *Proc. Geotechnical Conference, Oslo* **1**, 147-152.

Perrin, R M S (1971) *The Clay Mineralogy of British Sediments*. Mineralogical Society, London.

Skempton, A W & Petley, D J (1967) The strength along structural discontinuities in stiff clays. *Proc. Geotechnical Conference, Oslo*. **2**, 2-20.

**Table 1. Sample description.**

Church Farm, Shaftsbury, Dorset ST 855 223

## Borehole 1

Depth (m)	Mineral Sciences code	Description
9.80-9.82	GC19	Buff silty sand
10.00-10.02	GC20	Pale grey clayey silt
10.20-10.22	GC21	Pale grey clayey silt
10.40-10.42	GC22	Pale grey pyritic clay
10.53-10.55	GC23	Grey/green silty clay
10.58-10.60	GC24	Grey silty clay
10.60-10.61	GC25	Grey silty clay
----- <i>Shear plane</i>		
10.61-10.62	GC26	Grey silty clay
10.66-10.70	GC27	Dark grey silty pyritic clay
10.80-10.82	GC28	Dark grey silty pyritic clay

## Borehole 2

Depth (m)	Mineral Sciences code	Description
3.50	GC01	Orange brown silty sand
3.71	GC02	Orange brown silty sand
4.00	GC03	Orange brown silty sand
5.25	GC04	Orange brown clayey silty sand
5.67-5.69	GC05	Orange brown clayey silty sand
5.72-5.74	GC06	Orange brown silty clay
5.74-5.75	GC07	Grey black clay
----- <i>Shear plane</i>		
5.75-5.76	GC08	Grey black clay
5.80-5.84	GC09	Grey black silty clay
7.3	GC10	Grey black silty clay
9.00	GC11	Brown/grey clayey silty sand
11.00	GC12	Grey silty clay
12.20	GC13	Grey/brown silty clay
13.30	GC14	Grey/brown silty clay
14.00	GC15	Grey silty clay
15.00	GC16	Grey silty clay
17.00	GC17	Grey silty clay
18.00	GC18	Grey silty clay

Table 2. Borehole 1: Whole-rock and clay mineralogy.

Whole rock

<2 μm fraction

Sample	Quartz	Calcite	Pyrite	Other	Smectite	Mica	Kaolinite	Smectite	Mica	Kaolinite	Quartz	Cristobalite
GC19	****	tr	ND	feldspar (tr)	18	*	ND	****	**	tr	**	*
GC20	****	**	*	feldspar (tr)	17	*	tr	***	**	*	**	*
GC21	***	**	*	feldspar (tr)	18	*	tr	***	**	*	****	**
GC22	***	***	****		20	*	ND	***	**	*	****	**
GC23	***	***	tr		32	*	ND	***	**	*	***	*
GC24	**	***	*	feldspar (tr)	34	*	tr	***	**	*	***	*
GC25	***	***	*	feldspar (tr)	36	**	tr	***	**	*	***	*
GC26	***	***	tr		38	**	tr	***	**	*	***	*
GC27	***	***	tr		34	**	ND	***	**	*	***	*
GC28	***	**	tr	feldspar (tr)	33	*	tr	***	**	*	***	*

Relative X-ray intensities:

\*\*\*\* very strong  
 \*\*\* strong  
 \*\* medium  
 \* weak

tr trace  
 ND not detected

Smectite values derived from 2-ethoxyethanol surface area

Table 3. Borehole 2: Whole-rock and clay mineralogy.

Whole rock

<2 μm fraction

Sample	Quartz	Feldspar	Gypsum	Other	Smectite	Mica	Kaolinite	Smectite	Mica	Kaolinite	Quartz	Cristobalite
GC01	***	*	ND		14	*	ND	***	**	*	***	*
GC02	****	*	ND		5	*	ND	****	**	*	***	**
GC03	****	*	ND		7	*	ND	****	**	*	***	**
GC04	****	*	ND		16	**	ND	****	**	*	***	*
GC05	***	*	ND		16	**	ND	****	**	*	***	*
GC06	***	*	ND		20	*	ND	****	**	*	***	*
GC07	**	*	ND		31	*	ND	****	**	*	***	**
GC08	**	*	ND	pyrite (tr)	37	**	ND	****	***	*	***	*
GC09	**	*	ND		34	*	ND	****	***	*	***	**
GC10	**	*	*		21	tr	ND	****	**	*	**	*
GC11	***	*	tr	pyrite (tr)	23	*	tr	****	**	*	**	*
GC12	***	*	tr	calcite (tr) pyrite (tr)	20	**	tr	****	***	**	**	**
GC13	**	*	*		24	**	tr	****	***	**	*	**
GC14	**	*	*		27	**	tr	****	**	**	*	*
GC15	**	tr	tr	calcite (tr)	24	*	tr	****	**	***	*	*
GC16	**	tr	tr	pyrite (tr)	24	**	*	****	**	***	*	**
GC17	***	*	ND	pyrite (tr)	15	tr	*	****	**	***	*	*
GC18	***	tr	ND	pyrite (tr)	14	**	*	****	**	****	*	*

Relative X-ray intensities:

\*\*\*\* very strong  
 \*\*\* strong  
 \*\* medium  
 \* weak

tr trace  
 ND not detected

Smectite values derived from 2-ethoxyethanol surface area

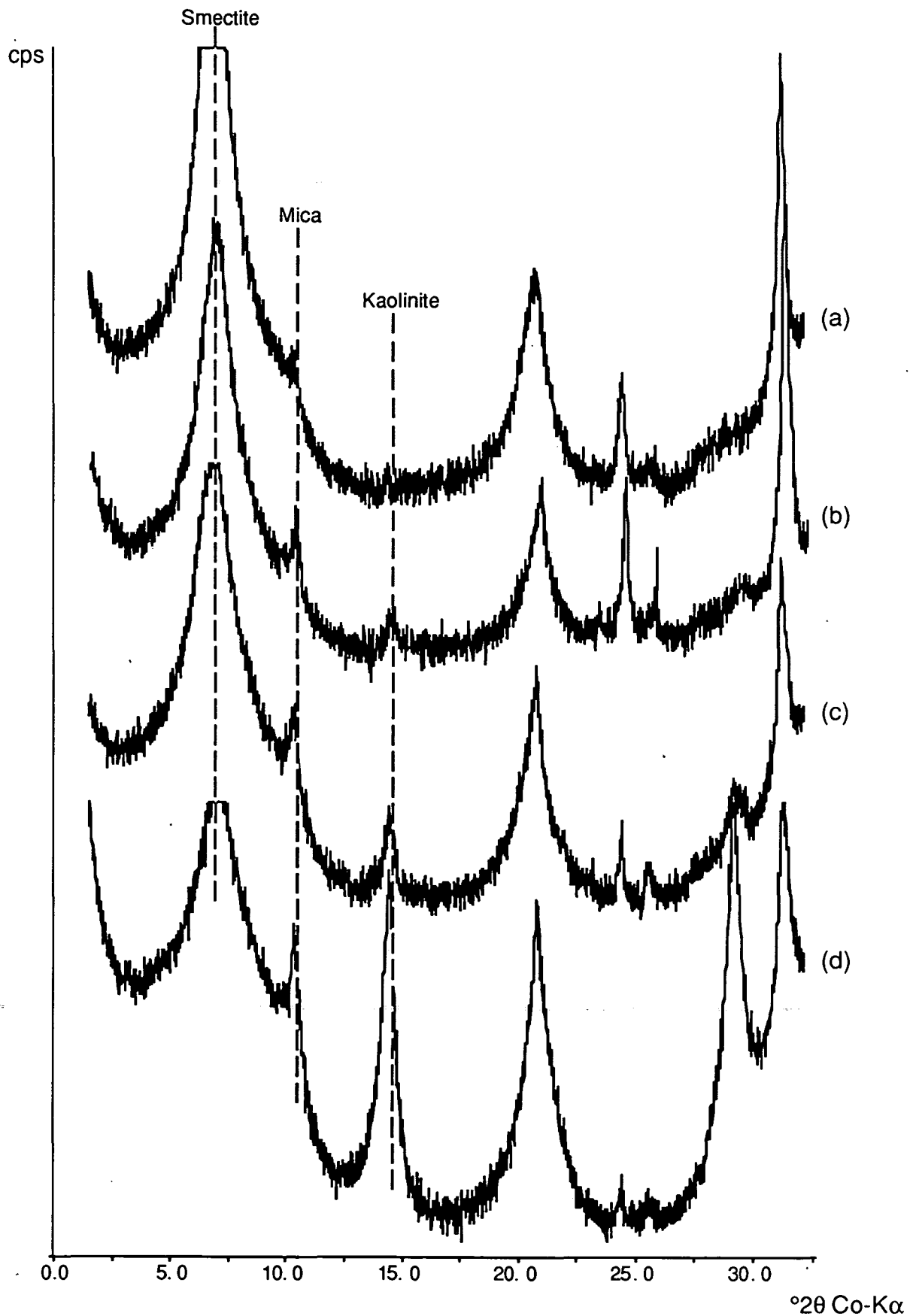
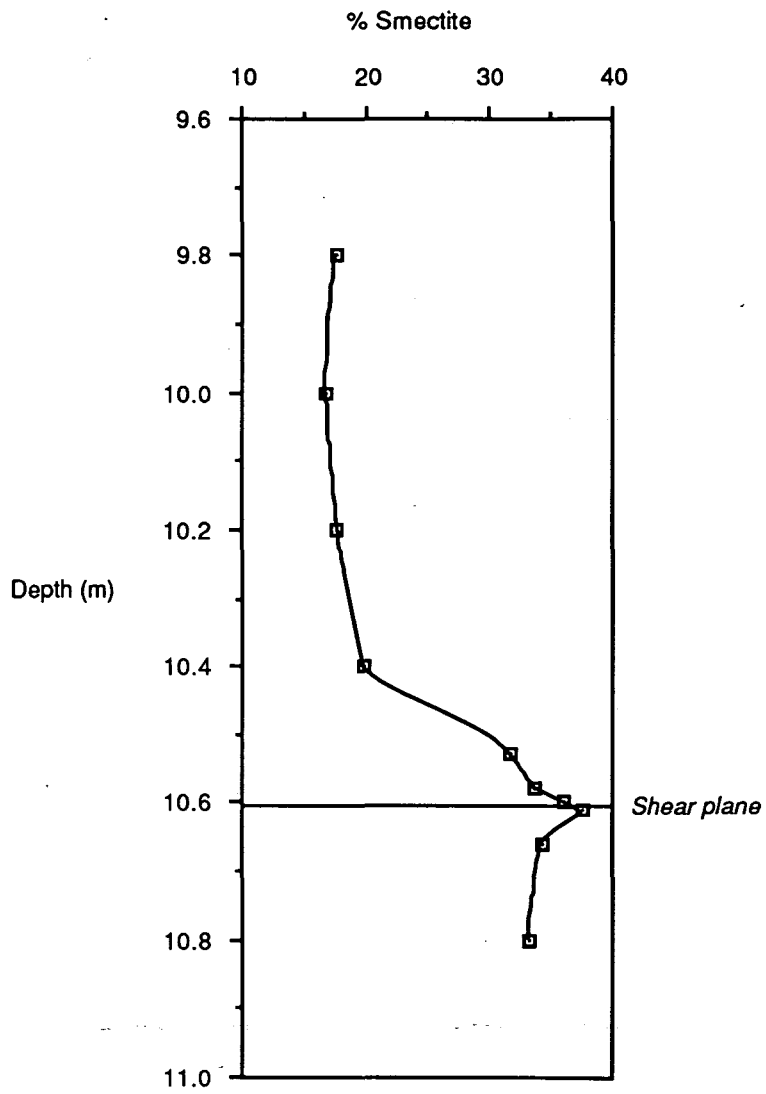


Figure 1. <math><2\ \mu\text{m}</math> air-dry oriented mount diffraction traces showing dominance of smectite in the clay mineral assemblage in the upper part of borehole 2 and relative increase in kaolinite content toward the base. (a) GC04 [5.50 m], (b) GC07 [5.74-5.75 m], (c) GC12 [11.00 m], (d) GC18 [18.00 m]



**Figure 2. Plot of smectite concentration against depth, borehole 1.**

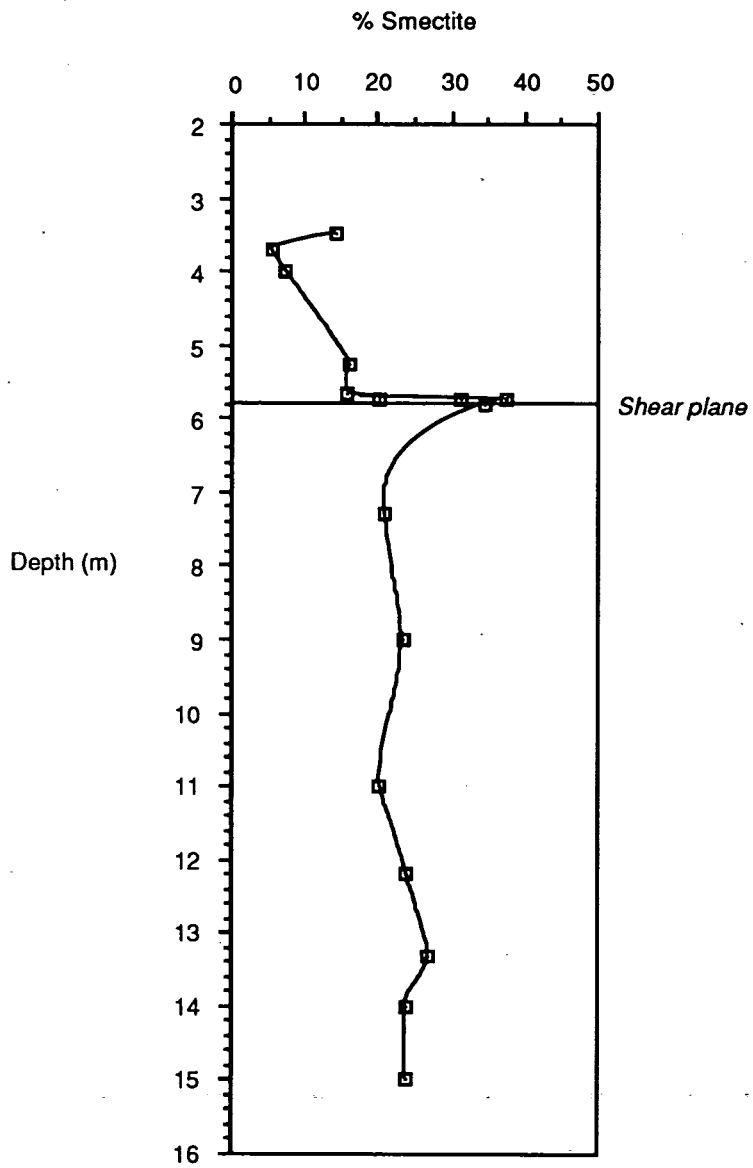


Figure 3. Plot of smectite concentration against depth, borehole 2.

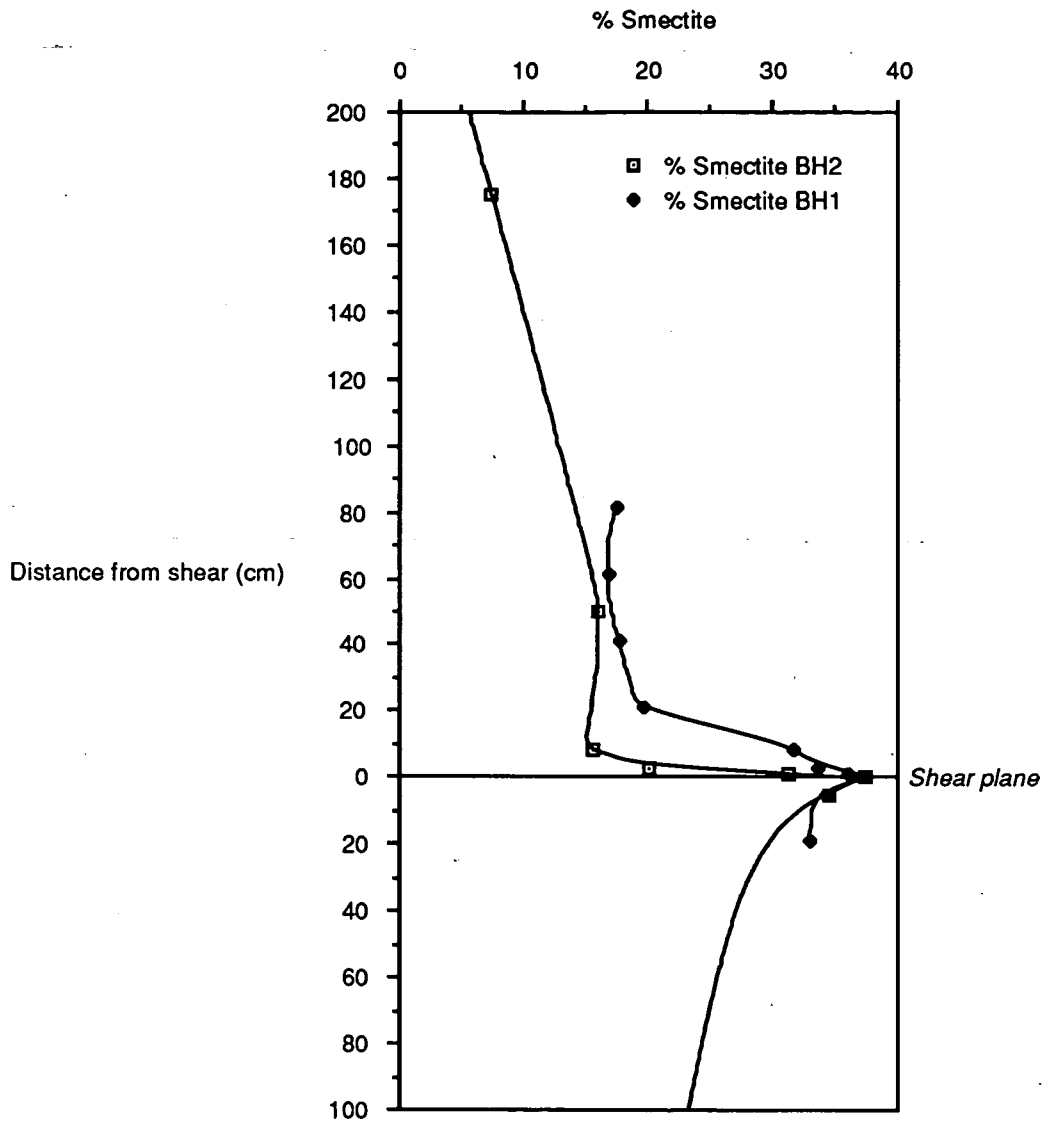
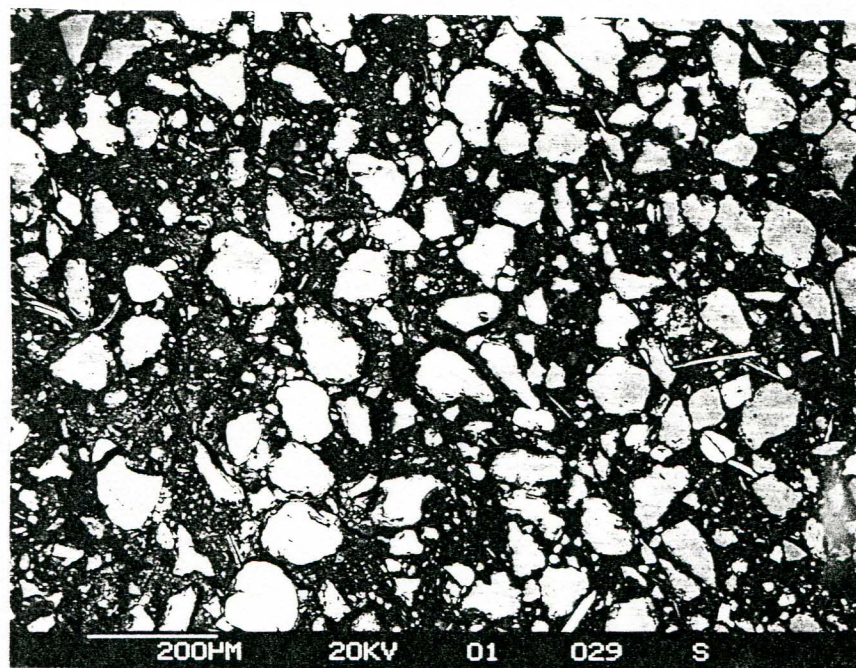


Figure 4. Plot of smectite concentration against distance from shear plane, boreholes 1 and 2.



**Plate 1. Undisturbed matrix-supported angular and sub-angular quartz grains with subordinate mica flakes, sponge spicules and sand-grade glauconite grains 8-10 mm above the estimated position of the shear zone in borehole 2.**

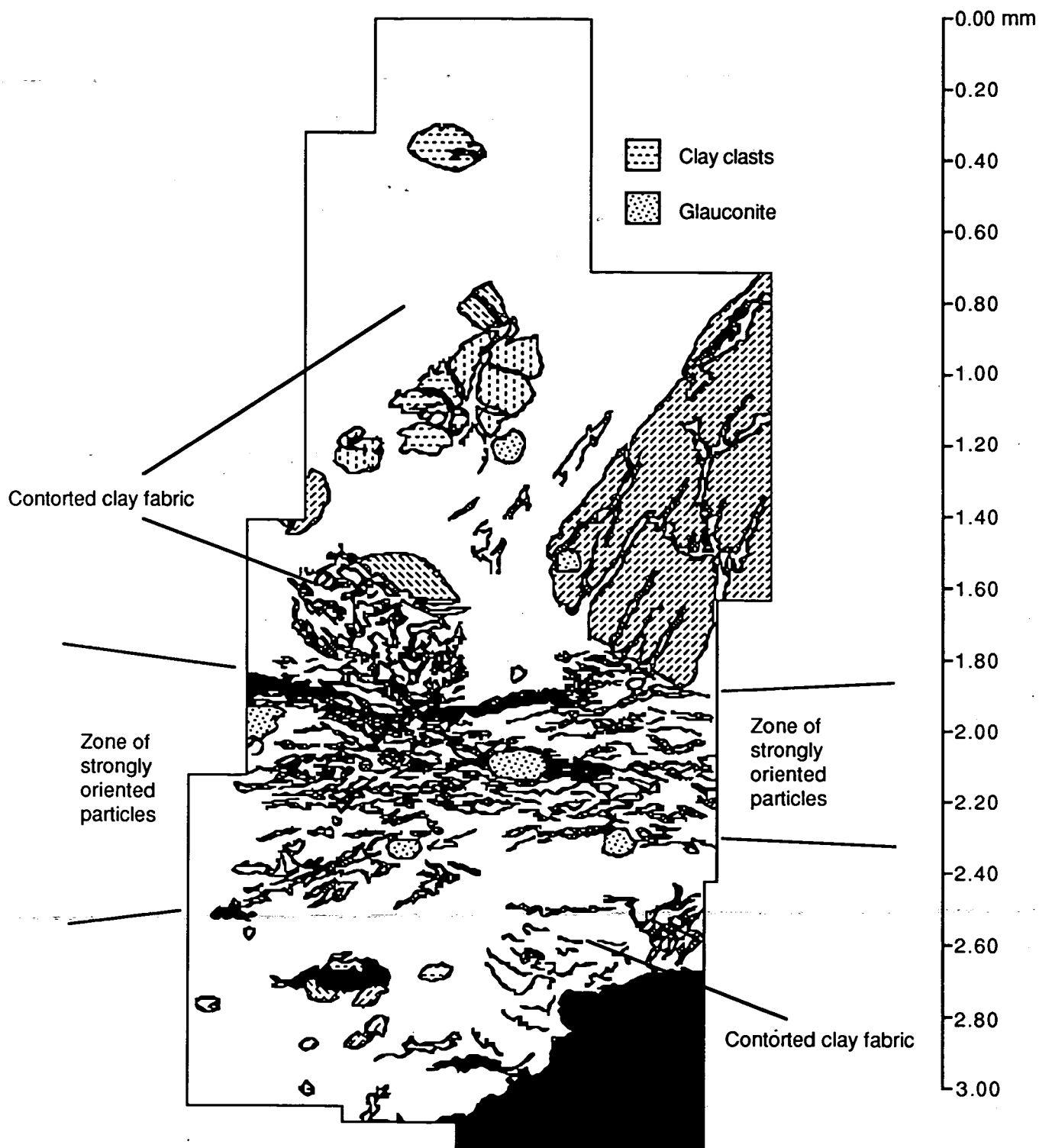


Figure 5. (above) Principal textural features in Plate 2 BSEM image composite Plate 2. (opposite) BSEM image composite of sheared mudrock from borehole 2

